



Potential parameters of PH₃ obtained by simultaneous fitting of ab initio data and experimental vibrational band origins

S.N. Yurchenko^{a,1}, M. Carvajal^a, Per Jensen^{a,*}, F. Herregodts^b, T.R. Huet^{b,2}

^a FB 9-Theoretische Chemie, Bergische Universität, D-42097 Wuppertal, Germany

^b Laboratoire de Physique des Lasers, Atomes et Molécules, Université des Sciences et Technologies de Lille, F-59655 Villeneuve d'Ascq cedex, France

Received 19 December 2002

Abstract

We report here the experimental observation, by photoacoustic spectroscopy, of transitions to the (600 A₁/E) local mode states of PH₃. The vibrational energies for these two states are used, together with all other experimentally derived vibrational energies for PH₃, as input for a least-squares refinement of the potential energy surface for the electronic ground state. We propose a procedure for simultaneously fitting the experimental data and ab initio values for the potential energy. By employing this procedure, we circumvent the problem of unrealistic behaviour of the fitted potential energy surface caused by the shortage of experimental data.

© 2003 Elsevier Science B.V. All rights reserved.

Keywords: PH₃; Vibrational spectra; Photoacoustic spectroscopy; Potential energy surface

1. Introduction

The present paper reports a procedure for refining an analytical representation of the potential energy surface by fitting to experimental data. The

initial values for the parameters of the analytical function are determined from ab initio values for the electronic energies, and we refine the potential energy surface by fitting simultaneously to these ab initio data and to vibrational energies determined experimentally.

It is well known that a fit to the experimental data alone can easily result in a significant distortion of the potential energy surface so that, for example, it would describe poorly the rotational spacings of the molecule. We eliminate this problem by requiring that the refined surface remain close to the initial ab initio one. Here, we apply the procedure to PH₃. We include in the input data for

* Corresponding author. Tel.: +49-202-439-2468; fax: +49-202-439-2509.

E-mail addresses: jensen@uni-wuppertal.de (P. Jensen), therese.huett@univ-lille1.fr (T.R. Huet).

¹ Present address: Steacie Institute for Molecular Sciences, National Research Council of Canada, Ottawa, Ont., Canada K1A 0R6.

² Also corresponding author.

the fitting the vibrational energies of the (600 A_1/E) local mode states measured by photoacoustic spectroscopy in the present work.

2. Experimental details

A photoacoustic spectrometer of high sensitivity ($\alpha_{\min} \sim 10^{-9} \text{ cm}^{-1}$) [1] was used to record the high resolution spectrum of the fifth P–H stretching overtone bands of phosphine. A titanium:sapphire ring laser (Model 899-29, Coherent) pumped by a 15 W cw Ar^+ laser (Innova 400) was coupled to an acoustic cell filled with the gas mixture at a pressure of 72 hPa. The laser beam was mechanically chopped at $f = 1370$ Hz for exciting the first longitudinal mode of the resonator. A Doppler-limited high resolution spectrum (Fig. 1) was recorded at room temperature in the region of $12\,500\text{--}12\,780 \text{ cm}^{-1}$ with the Autoscan II system attached to the laser. For the entire spectral range, the absolute calibration was checked with a Burleigh WA-1500 wavemeter, with an accuracy of 0.01 cm^{-1} . Around 200 transitions were assigned up to $J, K < 12$. The rovibrational structures of the upper states are described with a local model [2] by a set of 10 molecular parameters. The values of the other parameters are being held fixed to the ground state values [3]. The rms deviation of the fit is 0.012 cm^{-1} . The term values of the (600 A_1/E) states are almost degenerate ($12678.2130(48)$ and

$12678.2053(22) \text{ cm}^{-1}$, respectively); this is a manifestation of the local mode behavior of the P–H bonds. The details of the rotational analysis [4] will be published elsewhere.

3. Effective inversion–vibrational Hamiltonian

The vibrational Hamiltonian and the computer program XY3 for obtaining its eigenvalues have already been applied to the electronic ground state of NH_3 in [5]. The theoretical details will be published elsewhere [6].

The Hamiltonian is obtained in the Hougen–Bunker–Johns (HBJ) formalism [7]. In the HBJ approach, the vibrational motion of an XY_3 pyramidal molecule is described in terms of a non-rigid reference configuration following the inversion motion. The other (small amplitude) vibrations are described as displacements from this reference configuration. The theoretical model and the corresponding computer program XY3 are applicable to the isolated electronic states of any pyramidal XY_3 molecule independently of the height of the barrier to planarity. In [5] we applied the model to NH_3 whose barrier to planarity is low so that the energy splittings resulting from the tunneling through it are readily observable. In the present work, we apply the same model to PH_3 . For this molecule, the barrier to inversion is very high and tunneling does not take place on the time scale of the experiments delivering the data for our least squares fittings. It can be argued that in the high-barrier case, the special treatment of the inversion motion offered by the HBJ approach is not really required. We find it interesting and desirable, however, to unify the treatment of vibrational motion for as many molecules as possible, and so we have not developed a simpler, inversion-free model for PH_3 .

The construction of the vibrational kinetic energy operator employed in the present work was briefly outlined in [5]. It is expressed in terms of linearized internal coordinates. The coordinates used to parameterize it are given as Morse variables depending on the instantaneous values of the bond lengths r_i and their common equilibrium value r_e .

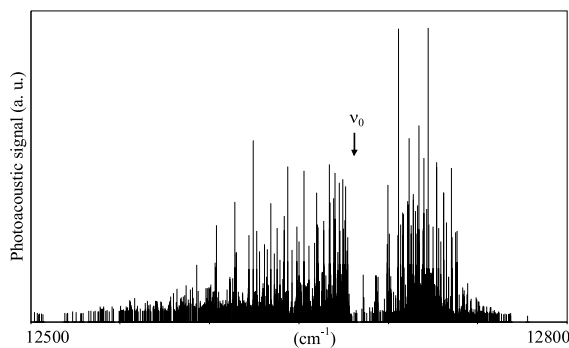


Fig. 1. Laser photoacoustic spectrum of the (600 A_1/E) overtone bands of PH_3 . The stick diagram displays the details of the rotational structure. At the scale of the figure the two band origins coincide at the position marked by ν_0 .

$$\xi_i = 1 - \exp(-a(r_i - r_e)), \quad i = 1, 2, 3, \quad (1)$$

where a is a molecular parameter, and the instantaneous interbond angles α_i (α_1 is the angle between r_2 and r_3 , α_2 is the angle between r_1 and r_3 , and α_3 is the angle between r_1 and r_2) are chosen in a symmetrized form

$$\xi_{4a} = \frac{1}{\sqrt{6}}(2\alpha_1 - \alpha_2 - \alpha_3), \quad (2)$$

$$\xi_{4b} = \frac{1}{\sqrt{2}}(\alpha_2 - \alpha_3) \quad (3)$$

together with the inversion coordinate ρ which, in the HBJ reference configuration, which has C_{3v} symmetry, is the angle between the C_3 axis and any one of the bonds. The coordinate ρ is defined in terms of Eckart and Sayvetz conditions; see, for example, Špirko [8]. The two coordinates (ξ_{4a} , ξ_{4b}) defined in Eqs. (2), (3) have E symmetry in the molecular symmetry group $C_{3v}(M)$ [9].

In order to get a better description of the potential surface and reduce the number of essential potential parameters, by analogy with the expansion used for triatomic molecules in [10], the analytical function used to represent the phosphine potential surface is chosen as

$$\begin{aligned} V(\xi_k; \sin \bar{\rho}) = & V_0(\sin \bar{\rho}) + \sum_j F_j(\sin \bar{\rho}) \xi_j \\ & + \sum_{j \leq k} F_{jk}(\sin \bar{\rho}) \xi_j \xi_k \\ & + \sum_{j \leq k \leq l} F_{jkl}(\sin \bar{\rho}) \xi_j \xi_k \xi_l \\ & + \sum_{j \leq k \leq l \leq m} F_{jklm}(\sin \bar{\rho}) \xi_j \xi_k \xi_l \xi_m + \dots, \end{aligned} \quad (4)$$

where the pure inversion potential function is determined as

$$V_0(\sin \bar{\rho}) = \sum_{s=1}^4 f_0^{(s)}(\sin \rho_e - \sin \bar{\rho})^s \quad (5)$$

and the expansion functions as

$$F_{jk\dots}(\sin \bar{\rho}) = \sum_{s=0}^n f_{jk\dots}^{(s)}(\sin \rho_e - \sin \bar{\rho})^s. \quad (6)$$

The integer n is chosen so that the ab initio data are well described with a potential of fourth order. The five curvilinear internal coordinates

ξ_k , $\{k = 1, 2, 3, 4a, 4b\}$ are defined in Eqs. (1)–(3) and

$$\sin \bar{\rho} = \frac{2}{\sqrt{3}} \sin\left(\frac{\alpha_1 + \alpha_2 + \alpha_3}{6}\right). \quad (7)$$

If the molecular geometry has C_{3v} symmetry, then it is easy to show that $\bar{\rho}$ is the angle between the C_3 axis and any one of the bonds. In less symmetrical configurations there is no simple geometrical interpretation of $\bar{\rho}$, but $\sin \bar{\rho}$ can be easily determined in any configuration [5]. The expansion coefficients $F_{jk\dots}(\sin \bar{\rho})$ depend on $\sin \rho_e - \sin \bar{\rho}$, where the parameter

$$\rho_e = \arcsin\left(\frac{2}{\sqrt{3}} \sin\left(\frac{\alpha_e}{2}\right)\right) \quad (8)$$

with α_e as the equilibrium value of any of the interbond angles. The first derivative for the potential energy function vanishes at planar geometries as required by symmetry and since $\sin \bar{\rho}$ is totally symmetric under the operations of the molecular symmetry group $D_{3h}(M)$ [9] of an XY_3 molecule with a low barrier to inversion (e.g., NH_3), it is also totally symmetric in $C_{3v}(M)$ [9], the molecular symmetry group of PH_3 .

Once the inversion–vibrational Hamiltonian is obtained (see [5]) the energy calculations are performed variationally. The vibration–inversion basis set is associated to the linearized coordinates to preserve the simplicity in the kinetic part. The basis functions are obtained as products of (a) Morse oscillator functions for the local stretching modes; (b) two-dimensional isotropic harmonic oscillator functions for the bending modes, and (c) inversion motion functions. The latter functions are obtained by numerically solving the one-dimensional inversion problem with the Numerov–Cooley approach [11–13]. To reduce the size of the final representation matrix it is “contracted” by prediagonalization of the zeroth order pure vibrational and inversion Hamiltonian separately.

4. The least-squares fitting of the potential energy surface

Modern high level ab initio calculations serve as a good starting point for analysis of experimental

spectroscopic information for polyatomic molecules. With an appropriate theoretical model, one can establish a connection between the internal molecular force field and observable experimental data. Thus, on one hand observable spectroscopic information can be predicted, and on the other hand the molecular structure can be elucidated.

In the present study we consider an approach for the refinement of the molecular potential energy surface (PES) from experimental values for the vibrational band centers. The PES of a molecule is normally represented by a parameterized, analytical function, and so it is defined by a set of values for the parameters in this function. The quality of the ab initio data is very often so good that theoretically calculated vibrational energies are very close to the experimental results, especially for small molecules. However, the accuracy of spectroscopic measurements is still significantly better than that of ab initio calculations, and so it is worthwhile to optimize the analytical representation of the PES by fitting potential parameters to the available experimental data. Even though a potential modified in this way may be very different from the “true” one and rather “effective,” it might play an important role in the analysis and prediction of spectra.

It is well known that the number of potential parameters N_p , that can be usefully varied in a least-squares fitting, is extremely restricted by the number of the available experimental data points N_{exp} . The formal requirement for the fitting to be possible is

$$N_p < N_{\text{exp}} \quad (9)$$

but in practice we will need $N_p \ll N_{\text{exp}}$ to carry out an acceptable fitting. However, in practice we often encounter the situation in which N_p is comparable to or even larger than N_{exp} . A reasonable description of the PES for a polyatomic molecule requires a large number of parameters N_p and the amount of observed data N_{exp} is generally limited.

A useful approach to increase the difference $N_{\text{exp}} - N_p$ is to employ theoretical relations between potential parameters. For example, the $x - K$ relations [14] can be used for local mode molecules; by introducing them we can replace Eq. (9) by

$$N_p - N_{\text{rel}} < N_{\text{exp}}, \quad (10)$$

where N_{rel} is the number of available relations. That allows one to increase substantially the number of parameters that can be varied.

Another, often used way of increasing $N_{\text{exp}} - N_p$ is to introduce constraints on the potential energy parameters. The simplest and most frequently used constraints fix some potential energy parameters either to zero or to their ab initio values. This reduces N_p in Eq. (9). It is obviously preferable to constrain to ab initio values if the available ab initio information is reliable.

Clearly, in carrying out a fitting of a given set of experimental data, we can find very many ways of constraining potential energy parameters, and many of these constraints will produce fittings of comparable accuracy. We will not be able to decide which of these fittings gives the best representation of the molecular PES since they reproduce the available experimental data equally well. These potential surfaces are “effective” and may have little similarity with the “true” PES.

We propose here to use the ab initio PES (which normally serves as a starting point for fittings of the type described here) as an additional source of input data for the optimization of the potential parameters to reproduce the observed energy differences. Assuming that the ab initio PES is close to the “true” surface within a known ab initio accuracy ϵ , we can force the refined PES not to deviate far from the ab initio one. Practically it is done by simultaneous fitting of the potential parameters to experimental data and to the ab initio data points. Instead of Eq. (9) we have the following formal condition

$$N_p < N_{\text{exp}} + N_{\text{points}}, \quad (11)$$

where N_{points} is a number of ab initio points. Eq. (11) immediately solves the problem of lack of the experimental data, since N_{points} is normally a large number. Moreover, an optimization of the potential function can be done even for one experimental value only!

If N_{points} is not large enough to ensure an acceptable determination of the PES parameters, we

can generate additional points by interpolation of the ab initio data. On the other hand, extrapolated PES points at higher energies can be used to control the behavior of the PES in asymptotic regions.

Two practical points must be mentioned here. First, the proposed approach involves the simultaneous fitting of data of different natures. We have to bring them into a proper relation by using appropriate weights. The weights control the extent to which we allow the fitted PES to deviate from the ab initio PES. Second, the initial ab initio points are not always available from the literature; it may be necessary to generate “pseudo”-ab initio points from published, analytical PES representations.

In the present study we apply the proposed approach to the optimization of the potential function for the electronic ground state of PH₃. Wang et al. [15] have studied this potential energy surface on different levels of theory with ab initio methods. Their best surface, which we adapt to our analytical expression given above, is our starting point for the refinement by fitting to experimental data.

The straight through calculation of the vibrational energies by the XY3 code [5] gives a root-mean-square (rms) deviation of 9.5 cm⁻¹ for the fundamental energy levels and 26.2 cm⁻¹ for all other measured vibrational energies (see the results given under the heading ‘ab initio’ in Table 2). However, the accuracy of the experimental data is assumed to be better than 10 cm⁻¹. We aim here to do band center calculations giving an rms deviation better than 10 cm⁻¹.

We extrapolated potential energy points up to 20 000 cm⁻¹ to ensure that the fit does not unreasonably destroy the shape of the ab initio potential energy surface. All points have associated weight factors as described below.

The PES geometries have been chosen randomly for 12 100 number of points. The bond lengths have been taken to lie in the range (1.20 Å, 1.62 Å) with an step of 0.01 Å. The interbond angles lie in the interval (80–115°) with a step of 1°.

Assuming that the ab initio PES provides higher accuracy in the vicinity of the equilibrium geometry, the whole grid of 12 100 points from 0

to 20 000 cm⁻¹ has been divided into two parts: Region I extends up to 3000 cm⁻¹ and comprises 9700 points, whereas the region II extends from 3000 cm⁻¹ to 20 000 cm⁻¹ and comprises 2400 points. The weight factors have been distributed from 10⁻² to 10⁻⁴ for Region I and from 10⁻⁴ to 10⁻⁶ for Region II so that the weight decreases with increasing energy. In this way, we force the fitted potential energy surface to remain close to the original ab initio surface in Region I. Larger deviations are allowed in Region II, but the points in this region serve to give the fitted PES a realistic shape.

The weight factors used for observed energies are listed in the Table 2; they are derived from the relative uncertainties of the measured data. The ratio between the potential-point weights W_i^{points} and the weight factors for the experimental energies W_i^{exp} is given as

$$R = \frac{\sum_{i=1}^{N_{\text{exp}}} W_i^{\text{exp}}}{\sum_{i=1}^{N_{\text{points}}} W_i^{\text{points}}}.$$

The value of $R = 3.2$, which has been found by trial and error, produces a fitting believed to reflect best the relative accuracy of ab initio information and experimental data, taking into account that the number of ab initio data points is vastly larger than that of measured vibrational energies.

The resulting optimized potential parameters are listed in Table 1, whereas the calculated vibrational energies are in Table 2. This table gives vibrational energy values only for the states that have been characterized experimentally; further predictions for states not observed are available from the authors on request. The rms deviation of the energies is now 1.1 cm⁻¹ for the fundamental levels and 4.8 cm⁻¹ for all other measured energies. The rms deviation for the potential point calculations is 6.9 cm⁻¹ for Region I and 40.0 cm⁻¹ for Region II. Thus, the optimized potential parameters (a) produce a PES close to the original ab initio one and (b) provide a reasonable qualitative behavior of the PES for large displacements from equilibrium. We note in Table 2 that even though, for example, the observed values for the (600 A₁/E) states are almost degenerate (12678.2130(48) and 12678.2053(22) cm⁻¹, respectively), which is a

Table 1
Potential energy parameters for the ground electronic state of PH₃ (in cm⁻¹)^a

	Ab initio	Fitted
f_0^2	297733 (65)	291474 (113)
f_0^3	-700833 (645)	-736350 (7236)
f_0^4	1923406 (8872)	1579581 (15844)
$f_1^1 = f_2^1 = f_3^1$	-13572.9 (86)	-13011 (86)
$f_1^2 = f_2^2 = f_3^2$	-3830 (162)	6828 (1841)
$f_{11}^0 = f_{22}^0 = f_{33}^0$	33579.9 (24)	33372.1 (55)
$f_{11}^1 = f_{22}^1 = f_{33}^1$	-3969 (44)	1023 (548)
$f_{11}^2 = f_{22}^2 = f_{33}^2$	-32882 (788)	-11530 (2555)
$f_{13}^1 = f_{12}^1 = f_{23}^1$	6333 (52)	3692 (755)
$f_{4a4a}^0 = f_{4b4b}^0$	18605.2 (26)	18864.9 (92)
$f_{4a4a}^1 = f_{4b4b}^1$	42695 (67)	36594 (814)
$\sqrt{\frac{3}{2}}f_{14a}^0 = -\sqrt{6}f_{24a}^0 = -\sqrt{6}f_{34a}^0 = \sqrt{2}f_{24b}^0 = -\sqrt{2}f_{34b}^0$	-1698.5 (27)	-1653 (26)
$\sqrt{\frac{3}{2}}f_{14a}^1 = -\sqrt{6}f_{24a}^1 = -\sqrt{6}f_{34a}^1 = \sqrt{2}f_{24b}^1 = -\sqrt{2}f_{34b}^1$	-24609 (86)	-6920 (1051)
$\sqrt{\frac{3}{2}}f_{14a}^2 = -\sqrt{6}f_{24a}^2 = -\sqrt{6}f_{34a}^2 = \sqrt{2}f_{24b}^2 = -\sqrt{2}f_{34b}^2$	-36258 (1597)	-76664 (27247)
$f_{111}^0 = f_{222}^0 = f_{333}^0$	-992 (13)	-1617 (94)
$f_{4a4a4a}^0 = -\frac{1}{3}f_{4a4b4b}^0$	2294 (57)	2470 (73)
$f_{4a4a4a}^1 = -\frac{1}{3}f_{4a4b4b}^1$	18155 (185)	-6786 (999)
$\sqrt{\frac{3}{2}}f_{114a}^0 = -\sqrt{6}f_{224a}^0 = -\sqrt{6}f_{334a}^0 = \sqrt{2}f_{224b}^0 = -\sqrt{2}f_{334b}^0$	-563 (15)	
$\sqrt{\frac{3}{2}}f_{114a}^1 = -\sqrt{6}f_{224a}^1 = -\sqrt{6}f_{334a}^1 = \sqrt{2}f_{224b}^1 = -\sqrt{2}f_{334b}^1$	-21974 (483)	184155 (3470)
$\sqrt{\frac{3}{2}}f_{234a}^0 = -\sqrt{6}f_{134a}^0 = -\sqrt{6}f_{124a}^0 = \sqrt{2}f_{134b}^0 = -\sqrt{2}f_{124b}^0$	-3382 (15)	-3134 (228)
$f_{14a4a}^0 = f_{24a4a}^0 = f_{34a4a}^0 = f_{14b4b}^0 = f_{24b4b}^0 = f_{34b4b}^0$	-6080.1 (64)	-5299 (57)
$\sqrt{\frac{3}{2}}f_{14a4a}^0 = -\sqrt{\frac{3}{2}}f_{14b4b}^0 = -\sqrt{6}f_{24a4a}^0 = -\sqrt{6}f_{34a4a}^0$ $= \sqrt{6}f_{24b4b}^0 = \sqrt{6}f_{34b4b}^0 = -\frac{1}{\sqrt{2}}f_{24a4b}^0 = \frac{1}{\sqrt{2}}f_{34a4b}^0$	3186.4 (86)	2500 (86)
$f_{1111}^0 = f_{2222}^0 = f_{3333}^0$	1865 (48)	3084 (110)
$f_{114a4a}^0 = f_{224a4a}^0 = f_{334a4a}^0 = f_{114b4b}^0 = f_{224b4b}^0 = f_{334b4b}^0$	-5069 (33)	-2223 (122)
$\sqrt{\frac{3}{2}}f_{114a4a}^0 = -\sqrt{\frac{3}{2}}f_{114b4b}^0 = -\sqrt{6}f_{224a4a}^0 = -\sqrt{6}f_{334a4a}^0$ $= \sqrt{6}f_{224b4b}^0 = \sqrt{6}f_{334b4b}^0 = -\frac{1}{\sqrt{2}}f_{224a4b}^0 = \frac{1}{\sqrt{2}}f_{334a4b}^0$	2770 (49)	-7341 (226)
$f_{234a4a}^0 = f_{134a4a}^0 = f_{124a4a}^0 = f_{234b4b}^0 = f_{134b4b}^0 = f_{124b4b}^0$	1190 (24)	-2501 (119)
$f_{4a4a4a4a}^0 = f_{4b4b4b4b}^0 = 1/2f_{4a4a4b4b}^0$	2332 (21)	2485 (58)
$f_{14a4a4a}^0 = f_{24a4a4a}^0 = f_{34a4a4a}^0 = -\frac{1}{3}f_{14a4b4b}^0 = -\frac{1}{3}f_{24a4b4b}^0$ $= -\frac{1}{3}f_{34a4b4b}^0$	-521 (14)	-688 (248)

^a The PES parameters ρ_c , r_c and a were fixed at their ab initio values $\rho_c = 122.7785^\circ$, $r_c = 1.411446 \text{ \AA}$ and $a = 1.6 \text{ \AA}^{-1}$.

well-known manifestation of local mode behaviour, the corresponding calculated values are not. They differ by 0.26 cm^{-1} . Similar deviations are seen for other pairs of local-mode states. The lack of degeneracy for the calculated energies is believed to be a consequence of lack of convergence in the theoretical calculation. The calculations reported here are carried out with the largest basis set which can be practically used with the computer available; it leads to matrix blocks with dimensions around 3000. Decreasing the size of the

basis set increases the differences between the local-mode energies. From the splitting of 0.26 cm^{-1} between the (600 A₁/E) energies we estimate that the level of convergence of the calculated energies in this region is on this order of magnitude.

The validity of the potential energy surface determined here is substantiated by the results obtained for PD₃ (Table 3). Even though the PD₃ energies were not used as input for the fitting, they are much better predicted with the fitted surface than with the original ab initio PES.

Table 2
Experimental and calculated vibrational energies of PH₃ (in cm⁻¹)

Γ	n ₁	n ₂	n ₃	N _b ^{l_b}	n ₆	Exp. ^a	Ab initio		Fitted		Weights
							Calc.	Obs.–Calc.	Calc.	Obs.–Calc.	
A ₁	0	0	0	0 ⁰	1	992.13	1000.62	-8.49	990.42	1.71	9.0
A ₁	0	0	0	0 ⁰	2	1972.55	1993.72	-21.17	1969.44	3.11	9.0
A ₁	0	0	0	2 ⁰	0	2226.83 ^b	2194.24	32.59	2228.66	-1.83	9.0
A ₁	1	0	0	0 ⁰	0	2321.12 ^b	2325.56	-4.44	2320.33	0.79	9.0
A ₁	0	0	0	0 ⁰	3	2940.77	2978.99	-38.22	2937.1	3.67	9.0
A ₁	0	0	0	2 ⁰	1	3214.2	3187.01	27.19	3212.84	1.36	9.0
A ₁	1	0	0	0 ⁰	1	3305.8	3322.68	-16.88	3306.5	-0.7	9.0
A ₁	0	0	0	0 ⁰	4	3896.02	3955.67	-59.65	3893.04	2.98	9.0
A ₁	1	0	0	0 ⁰	2	4282.4	4312.46	-30.06	4281.74	0.66	9.0
A ₁	2	0	0	0 ⁰	0	4566.26	4565.74	0.52	4564.6	1.66	5.0
A ₁	1	1	0	0 ⁰	0	4644.66	4650.27	-5.61	4644.51	0.15	5.0
A ₁	2	0	0	0 ⁰	2	6503.1	6551.14	-48.04	6503.21	-0.11	5.0
A ₁	3	0	0	0 ⁰	0	6714.60	6724.09	-9.49	6718.33	-3.73	5.0
A ₁	2	1	0	0 ⁰	0	6881.53	6890.06	-8.53	6882.5	-0.97	1.0
A ₁	1	1	1	0 ⁰	0	6971.16	6972.86	-1.7	6971.22	-0.06	1.0
A ₁	2	1	0	1 ¹	0	7961.9	7947.71	14.19	7962.73	-0.83	1.0
A ₁	4	0	0	0 ⁰	0	8788.0	8768.31	19.69	8785.52	2.48	0.5
A ₁	3	1	0	0 ⁰	0	9040.0	9046.01	-6.01	9043.75	-3.75	0.5
A ₁	6	0	0	0 ⁰	0	12678.21 ^c	12610.9	67.31	12680.75	-2.54	0.1
E	0	0	0	1 ¹	0	1118.31	1101.98	16.33	1117.92	0.39	9.0
E	0	0	0	1 ¹	1	2108.15 ^b	2098.78	9.37	2106.68	1.47	9.0
E	0	0	0	2 ²	0	2234.93 ^b	2198.59	36.34	2232.1	2.83	9.0
E	1	0	0	0 ⁰	0	2326.87 ^b	2325.62	1.25	2326.54	0.33	9.0
E	1	0	0	1 ¹	0	3423.9	3416.78	7.12	3426.05	-2.15	9.0
E	2	0	0	0 ⁰	0	4565.78	4566.08	-0.3	4565.89	-0.11	5.0
E	2	0	0	0 ⁰	1	5540.0	5562.45	-22.45	5539.63	0.37	5.0
E	2	0	0	1 ¹	0	5645.4	5648.73	-3.33	5644.22	1.18	5.0
E	3	0	0	0 ⁰	0	6714.60	6720.25	-5.65	6714.97	-0.37	5.0
E	2	1	0	0 ⁰	0	6883.73	6887.37	-3.64	6885	-1.27	1.0
E	2	1	0	0 ⁰	0	6890.86	6889.44	1.42	6890.28	0.58	1.0
E	3	0	0	0 ⁰	1	7679.1	7701.34	-22.24	7672.55	6.55	1.0
E	3	0	0	1 ¹	0	7775.5	7714.97	60.53	7772.24	3.26	1.0
E	2	1	0	1 ¹	0	7961.9	7948.36	13.54	7961.27	0.63	1.0
E	4	0	0	0 ⁰	0	8788.0	8756.03	31.97	8795.6	-7.6	0.5
E	3	1	0	0 ⁰	0	9040.0	9043.44	-3.44	9045.24	-5.24	0.5
E	6	0	0	0 ⁰	0	12678.21 ^c	12613.2	65.01	12681.01	-2.80	0.1

^a Ref. [16].

^b Ref. [17].

^c From this work.

5. Conclusion

In refining the potential energy surface for the electronic ground state of PH₃, we face the usual problem that we have many parameters and just a few experimental values to be used as input for the fitting. The customary solution to this problem would be to constrain some of the parameter values, either to zero or to the ab initio values. The

typical situation is that with different constraints, we get different fittings with comparable standard deviations. That is, we cannot distinguish between these fits and choose the best one, unless we have some criterion for choosing such as a comparison between experimental and theoretical intensity values. So we may be able to find as many potential energy surfaces as we can find ways of constraining the parameters. These surfaces are

Table 3
Experimental and calculated vibrational energies of PD₃ (in cm⁻¹)

Γ	n_1	n_2	n_3	N_b^{lb}	n_6	Exp. ^a	Ab initio		Fitted	
							Calc.	Obs.–Calc.	Calc.	Obs.–Calc.
A ₁	0	0	0	0 ⁰	1	728.28	732.42	-4.14	724.8	3.48
A ₁	0	0	0	0 ⁰	2	1442.0	1460.84	-18.84	1443.43	-1.43
A ₁	1	0	0	0 ⁰	0	1682.11	1686.14	-4.03	1682.23	-0.12
A ₁	0	0	0	0 ⁰	3	2155.0	2185.26	-30.26	2155.99	-0.99
A ₁	0	0	0	0 ⁰	4	2860.0	2905.55	-45.55	2862.47	-2.47
E	0	0	0	1 ¹	0	803.14	795.34	7.8	804.98	-1.84
E	1	0	0	0 ⁰	0	1693.3	1694.81	-1.51	1693.79	-0.49

^a Ref. [18].

“effective” and they may be very different from the “true” surface. One way out of this dilemma is to note that presumably the ab initio surface, which we aim at refining, is realistic. Thus we should prevent the fitted surface from distorting wildly away from the ab initio surface. In the case of PH₃ considered here we have experimental vibrational data up to 13 000 cm⁻¹. Fitting the potential energy surface using different constraints would provide surfaces reliable in this energy region. At higher energies, the fitted surface would probably be unrealistic.

In practice, we can obtain a realistic potential energy surface in the following way: once we have values of the potential energy parameters, we can calculate the potential energy at any geometry, or we can calculate any vibrational energy. Thus, we can fit these quantities simultaneously. The two types of data are of different nature and we must weight them appropriately in the fitting. By this weighting, we “tie” the fitted potential energy function to the ab initio points. We have applied the proposed procedure to fitting the potential energy surface for the electronic ground state for PH₃ and have improved the agreement between theory and experiment for the vibrational energies not only for PH₃, but also for PD₃ whose vibrational energies were not included in the input for the fitting. We included in the input data for the fitting the vibrational energies of the (600 A₁/E) local mode states of PH₃ measured by photoacoustic spectroscopy in the present work. The fitted potential energy function is rather close to the original ab initio one, the rms deviation between

the two surfaces (calculated in the points used as input for the fitting) is 39.8 cm⁻¹.

Acknowledgements

This work is supported by the European Commission through Contract No. HPRN-CT-2000-00022 “Spectroscopy of Highly Excited Rovibrational States”.

References

- [1] S. Tranchart, I. Hadj Bachir, T.R. Huet, A. Olafsson, J.-L. Destombes, S. Naïm, A. Fayt, *J. Mol. Spectrosc.* 196 (1999) 265.
- [2] H. Bürger, M. Lecoutre, T.R. Huet, J. Breidung, W. Thiel, V. Hänninen, L. Halonen, *J. Chem. Phys.* 114 (2001) 8844.
- [3] L. Fusina, G. Dilonardo, *J. Mol. Struct.* 517 (2000) 67.
- [4] F. Herregodts, W. Jerzembeck, T.R. Huet, in: 17th International Conference on High Resolution Molecular Spectroscopy, Abstract J47, Prague, Czech Republic (2002).
- [5] H. Lin, W. Thiel, S.N. Yurchenko, M. Carvajal, P. Jensen, *J. Chem. Phys.* 117 (2002) 11265.
- [6] S.N. Yurchenko, M. Carvajal, P. Jensen, in preparation.
- [7] J.T. Hougen, P.R. Bunker, J.W.C. Johns, *J. Mol. Spectrosc.* 34 (1970) 136.
- [8] V. Špirko, *J. Mol. Spectrosc.* 101 (1983) 30.
- [9] P.R. Bunker, P. Jensen, *Molecular Symmetry and Spectroscopy*, NRC Research Press, Ottawa, 1998, second ed.
- [10] P. Jensen, *J. Mol. Spectrosc.* 128 (1988) 478.
- [11] D. Papoušek, J.M.R. Stone, V. Špirko, *J. Mol. Spectrosc.* 48 (1973) 17.
- [12] P. Jensen, *Computer Physics Reports* 1 (1983) 1.

- [13] J.W. Cooley, *Math. Comput.* 15 (1961) 363.
- [14] J.E. Baggot, *Mol. Phys.* 65 (1988) 739.
- [15] D. Wang, Q. Shi, Q.-S. Zhu, *J. Chem. Phys.* 112 (2000) 9624.
- [16] S.-G. He, J.-J. Zheng, S.-M. Hu, H. Lin, Y. Ding, X.-H. Wang, Q.-S. Zhu, *J. Chem. Phys.* 114 (2001) 7018.
- [17] O.N. Ulenikov, E.S. Bekhtereva, V.A. Kozinskaia, J.-J. Zheng, S.-G. He, S.-M. Hu, Q.-S. Zhu, C. Leroy, L. Pluchart, *J. Mol. Spectrosc.* 215 (2002) 295.
- [18] S. Civiš, P. Čarský, V. Špirko, *J. Mol. Spectrosc.* 118 (1981) 88.